Modeling of the magnetic free energy of self-diffusion in bcc Fe

N. Sandberg,[1,2,*] Z. Chang,[1,†] L. Messina,[1] P. Olsson,[1] and P. Korzhavyi[3]

[1]*KTH Royal Institute of Technology, Reactor Physics, Roslagstullsbacken 21, SE-10691 Stockholm, Sweden*

[2]*Swedish Radiation Safety Authority, SE-171 16 Stockholm, Sweden*

[3]*KTH Royal Institute of Technology, Department of Materials Science and Engineering, Brinellvägen 23, SE-10044 Stockholm, Sweden*

(Received 11 June 2015; revised manuscript received 27 September 2015; published 6 November 2015)

A first-principles based approach to calculating self-diffusion rates in bcc Fe is discussed with particular focus on the magnetic free energy associated with diffusion activation. First, the enthalpies and entropies of vacancy formation and migration in ferromagnetic bcc Fe are calculated from standard density functional theory methods in combination with transition state theory. Next, the shift in diffusion activation energy when going from the ferromagnetic to the paramagnetic state is estimated by averaging over random spin states. Classical and quantum mechanical Monte Carlo simulations within the Heisenberg model are used to study the effect of spin disordering on the vacancy formation and migration free energy. Finally, a quasiempirical model of the magnetic contribution to the diffusion activation free energy is applied in order to connect the current first-principles results to experimental data. The importance of the zero-point magnon energy in modeling of diffusion in bcc Fe is stressed.

DOI: 10.1103/PhysRevB.92.184102 PACS number(s): 75.50.Bb, 75.20.−g, 75.10.−b, 66.30.Fq

I. INTRODUCTION

Self-diffusion and substitutional impurity diffusion in metals have been treated based on first-principles methods in a number of recent papers [1–8]. In many cases, good quantitative agreement is obtained between calculations and experiments both in terms of activation energies and absolute diffusion rates. In body centered cubic (bcc) Fe, a purely theoretical approach to calculating the diffusion rate $D(T)$ as a function of temperature T is hindered by the complications associated with the magnetic transition occurring at the Curie temperature T_C. The apparent activation energy Q varies both below and above T_C, due to magnetic disordering. Therefore, in order to describe self-diffusion and impurity diffusion in Fe, the magnetic free energy $G_a^{mag}(T)$ associated with diffusion activation (vacancy formation and atom-vacancy exchange) must be modeled. A number of approximate or semiempirical models for G_a^{mag} have been suggested in the literature and then used in fitting to experimental data, see Ref. [9] and references therein. Recent theoretical developments have made it possible to treat not only the magnetically ordered states but also disordered states in calculating the relevant activation enthalpies from first principles [7]. In other words, the difference $\Delta Q^{FM\to PM} \equiv Q^{PM} - Q^{FM}$ between the ferromagnetic (FM) and the paramagnetic (PM) states can be calculated. However, in order to predict absolute diffusion rates, the full temperature dependence of $G_a^{mag}(T)$ must be known. Reversely, if an assumed form for $G_a^{mag}(T)$ is used in fitting to experimental data, extrapolations, e.g., to low temperatures, may be misleading.

In the current paper we focus on the modeling of $G_a^{mag}(T)$ for the temperature range from 0 K to the fully disordered state. While the prediction of diffusion parameters (prefactors and activation energies) is relatively straightforward in nonmagnetic metals or in magnetic materials well below T_C, it is considerably more challenging to take magnetic disordering into account. Achieving a purely theoretical description of the magnetic free energy has proven very difficult even in bulk Fe [10]. It is therefore expected to be no less difficult in the modeling of diffusion, since the free energies of interest are now defined per vacancy, or per activated state, with the bulk free energy subtracted.

The magnetic free energy consists of an enthalpy and an entropy part $G^{mag}(T) = H^{mag}(T) - T\,S^{mag}(T)$. In our current approach we estimate $G_a^{mag}(T)$ for temperatures ranging from zero to the melting temperature in the following steps. First, we estimate $\Delta Q^{FM\to PM}$ directly from first-principles density functional theory (DFT) calculations by averaging over a large number of supercell calculations in which the local magnetic moments are randomly set. That is done for bulk, vacancy, and transition state structures, respectively. Second, the temperature variation of G_a^{mag} is studied within a Heisenberg model by means of classical and quantum Monte Carlo (MC) simulations. In this approach, the magnetic properties of bcc Fe are described by the interaction of localized spins with spin quantum number $S = 1$. This approximation works surprisingly well, e.g., T_C is predicted to within 10%. However, in an accurate description of the magnetic free energy in Fe one should account for the fact that the effective spin interactions are dependent on the global spin order. Lacking such a more elaborate model of $G_a^{mag}(T)$ we proceed to evaluate two semiempirical models used in the literature against our MC data. Based on that comparison, we can link experimental data on bulk magnetic enthalpies to a model of $G_a^{mag}(T)$ which is then linked to our first-principles calculations. The result is critically compared with experimental and theoretical estimates of the vacancy formation and diffusion free energies in bcc Fe. Thus, the aim of the current work is not to present a completely theoretical route to calculating diffusion rates in magnetic metals and alloys, but rather to investigate separately the magnetic terms, in order to point out problems that should be addressed in future work.

*nilssa@kth.se

†zhongwen@kth.se

Our paper is structured as follows. Some basic theory and a discussion of different models of the magnetic free energy associated with diffusion are presented in Sec. II. In Sec. III the computational methods based on first-principles DFT, and on Heisenberg model MC simulations, are described. The results are presented and discussed in Sec. IV, and the paper ends with conclusions, Sec. V.

II. RATE THEORY OF DIFFUSION

The current modeling of vacancy-mediated diffusion is based on standard lattice dynamics theory and transition state theory (TST) [11,12]. In TST, the rate of vacancy migration is related to the partition function in the $3N-1$ dimensional hypersurface defining the transition state (TS). For tracer diffusion in a pure crystal one then has

$$D_{\rm tr}(T) = \tfrac{1}{6} l^2 z \nu_0 f_{\rm c} \exp\{-[G_{\rm f}(T) + G_{\rm m}(T)]\}/k_{\rm B}T, \qquad (1)$$

where $z = 8$ is the coordination number for the bcc structure, l is the jump length, ν_0 is an attempt frequency, $f_{\rm c} = 0.72$ is the correlation factor in bcc, and $k_{\rm B}$ is the Boltzmann constant. The Gibbs free energies of vacancy formation and migration $G_{\rm f}$ and $G_{\rm m}$ can each be expressed in terms of the corresponding enthalpy H and entropy S: $G = H - TS$.

For convenience we restate Eq. (1) as

$$D_{\rm tr} = D_0 \exp\{-[Q^{\rm FM} + Q_2 T^2 + G^{\rm mag}(T) - \Delta Q^{\rm FM\to PM}]/k_{\rm B}T\}. \qquad (2)$$

Each term in the exponent refers to a sum of vacancy formation and migration terms, e.g., $Q^{\rm FM} = H_{\rm f}^{\rm FM} + H_{\rm m}^{\rm FM}$. The activation energy in the FM region is assumed to consist of a static part $Q^{\rm FM}$, as obtained in standard DFT calculations, and a second-order term Q_2 to be discussed further on. Entropy factors present in the FM region (vibrational and electronic) are collected in the prefactor D_0, while the magnetic free energy is kept in the exponent. The term $\Delta Q^{\rm FM\to PM}$ is added because the paramagnetic state is conveniently used as reference for the magnetic terms.

A thermodynamic property associated with vacancy formation is defined as the difference between the systems with and without a vacancy,

$$X_{\rm f} = X^{\rm vac} - \frac{N-1}{N} X^{\rm bulk}, \qquad (3)$$

where N is the number of atoms in the bulk system. Similarly, a thermodynamic property associated with vacancy migration is defined as the difference between the system constrained at the TS and the vacancy state,

$$X_{\rm m} = X^{\rm TS} - X^{\rm vac}. \qquad (4)$$

Then, for thermally activated diffusion one has

$$X_{\rm a} = X^{\rm TS} - \frac{N-1}{N} X^{\rm bulk}. \qquad (5)$$

The diffusion activation enthalpy is in bcc materials usually found to be temperature dependent, which may be partly due to electronic excitations, and partly to anharmonic lattice vibrations [5]. Here we assume that a static and a second order term, in addition to the magnetic term, are sufficient to describe vacancy formation and migration,

$$H(T) = H_0 + H_2 T^2 + H^{\rm mag}(T). \qquad (6)$$

A. The magnetic free energy

In the following section, a quasiempirical model of the magnetic free energy of vacancy formation and migration is presented. The bulk magnetic thermal capacity per atom is written $c(\tau)$, where $\tau = T/T_{\rm C}$. Next, it is assumed that for a vacancy concentration $x \ll 1$, the thermal capacity curve is scaled according to

$$c(x,\tau) = (1-x)c\left(0, \frac{\tau}{1-\gamma x}\right). \qquad (7)$$

With $\gamma = 1$, this model accounts for the effect of "dilution" by removing magnetic couplings. With γ smaller or larger than unity, the additional effect of strengthening or weakening of the magnetic couplings of the surrounding lattice is accounted for. The magnetic moments themselves are assumed to be unaffected in this model. Application of the thermodynamic relation $c = dh/d\tau = \tau ds/d\tau$ leads to

$$h(x,\tau) = (1-x)(1-\gamma x)h\left(0, \frac{\tau}{1-\gamma x}\right) \qquad (8)$$

and

$$s(x,\tau) = (1-x)s\left(0, \frac{\tau}{1-\gamma x}\right) \qquad (9)$$

for the enthalpy and entropy, respectively. The corresponding magnetic free energy is

$$g(x,\tau) = (1-x)(1-\gamma x)g\left(0, \frac{\tau}{1-\gamma x}\right). \qquad (10)$$

The free energy per vacancy is defined by

$$G_{\rm f}^{\rm mag}(\tau) = \lim_{x\to 0}\left[\frac{\partial}{\partial x} g(x,\tau) - (1-x)g(0,\tau)\right], \qquad (11)$$

where we now use capital letters for properties expressed per vacancy, or per activated state. The above equation corresponds to the $N \to \infty$ limit of Eq. (3). This leads to

$$G_{\rm f}^{\rm mag}(\tau) = -\gamma g(0,\tau) + \gamma \tau g'(0,\tau) \qquad (12)$$

or

$$G_{\rm f}^{\rm mag}(\tau) = -\gamma h(0,\tau). \qquad (13)$$

The above discussion was focused on the formation of vacancies. In the modeling of diffusion, one also has to take the migration free energy $G_{\rm m}^{\rm mag}$ into account. A simple bond-cutting argument [13] leads to the expectation that the free energy of diffusion should vary in the same way as that of vacancy formation, but with a slightly higher prefactor, i.e., $G_{\rm a}^{\rm mag} = -\gamma_{\rm a} h(0,\tau)$, with $\gamma_{\rm a} \approx \frac{5}{4}\gamma$. Explicit calculations taking into account the distance dependence of magnetic interactions are presented in the current paper.

Girifalco arrived at $G_{\rm f}^{\rm mag}(\tau) = -h(\tau)$ based on a rigorous statistical mechanics treatment within a mean-field approach [14] and in generalizations to quasichemical theory [15]. Braun and Feller-Kniepmeier [16] assumed an expression similar to Eq. (13) to hold with $h(0,\tau)$ connected to the magnetization curve via mean-field theory and γ taken as a fitting parameter.

The formation of a vacancy can be seen as the introduction of a nonmagnetic solute atom, and therefore the theory of magnetic alloys can be applied. In this field, a different treatment has been used [17], originating with the work of Zener [18]. A shift of $g(\tau)$ along the temperature and free-energy axes is assumed, leading to the following free energy:

$$G_{\mathrm{f}}^{\mathrm{mag}}(\tau) = \Delta T_{\mathrm{X}}[s(0,\tau) - s^{\mathrm{PM}}], \tag{14}$$

where ΔT_{X} measures the rate of shifting as a function of solute concentration. Thus, one finds that by shifting along the temperature axis, the magnetic free energy varies as the bulk magnetic *entropy*.

We have found that in fitting to self-diffusion data in bcc Fe, it is not of crucial importance, in a numerical sense, whether the scaling model or the Zener model is applied in combination with some model of the magnetization curve. However, the scaling model has the advantage of being more straightforward to connect to theoretical calculations. By a derivation similar to the one above for the vacancy formation free energy, one arrives at $Q = -\gamma_{\mathrm{a}}[h(0,\tau) - \tau c(0,\tau)]$, and by taking the high-temperature and low-temperature limits,

$$\Delta Q^{\mathrm{FM}\to\mathrm{PM}} = -\gamma_{\mathrm{a}} \Delta h^{\mathrm{FM}\to\mathrm{PM}}, \tag{15}$$

where $\Delta h^{\mathrm{FM}\to\mathrm{PM}} \equiv h^{\mathrm{PM}} - h^{\mathrm{FM}}$. In other words, the scaling model allows the parameter γ_{a} to be deduced directly from theoretical estimates of the disordering enthalpy associated with diffusion activation.

III. COMPUTATIONAL METHODS

A. First-principles calculations in the ferromagnetic state

Our first-principles calculations were performed within the framework of the Kohn-Sham density functional theory (DFT) implemented in the Vienna *ab initio* simulation package (VASP) code [19–23]. The projector augmented wave (PAW) method was used in the frozen core approximation, and the Perdew-Burke-Ernzerhof (PBE) generalized-gradient approximation (GGA) was used as electronic exchange correlation function. All calculations were performed with a cutoff energy of 350 eV, and a Monkhorst-Pack k-point mesh of $3 \times 3 \times 3$ was used unless otherwise specified. The method of Methfessel and Paxton of order 2 was used with a smearing width of 0.3 eV. Supercells of 54 or 128 ($3 \times 3 \times 3$ and $4 \times 4 \times 4$ conventional bcc unit cells) were used, with periodic boundary conditions.

Structural relaxations of bulk, vacancy, and transition state systems were carried out, with allowance of cell shape change and cell volume change. The vacancy formation and migration energies were then obtained in accordance with Eqs. (3) and (4).

Frozen-phonon calculations [24] were used to obtain the pre-exponential factor D_0. Starting from the relaxed supercells, small displacements were applied to each atom in five steps between ± 0.03 Å around the equilibrium position. Force constants were fitted to the resulting forces and inserted into the force constant matrix from which the eigenfrequencies ν are obtained by diagonalization. In these calculations, the system is in the FM state, and the influence of magnetic disordering on the phonon frequencies is not modeled.

From standard lattice dynamics theory, the vibrational entropy associated with vacancy formation is given in terms of the eigenfrequencies ν of bulk and vacancy systems as

$$S_{\mathrm{f}} = -k_{\mathrm{B}}\left[\sum \ln(\nu^{\mathrm{vac}}) - \frac{N-1}{N}\sum \ln(\nu^{\mathrm{bulk}})\right]. \tag{16}$$

The vacancy jump frequency is given by the related expression [12]

$$\nu_{\mathrm{m}} = z\frac{\prod_{j=1}^{3N-4}\nu_j^{\mathrm{vac}}}{\prod_{j=1}^{3N-3}\nu_j^{\mathrm{TS}}}\exp(-H_{\mathrm{m}}/k_{\mathrm{B}}T). \tag{17}$$

By combining Eqs. (16) and (17), the prefactor in the fully ordered ferromagnetic state D_0 is readily found.

As previously mentioned, the formation and migration enthalpies are expected to contain a second-order term in T due to electronic excitations and anharmonic lattice vibrations. Here we estimate the electronic part as follows. In the independent-electron approximation and for a static density of states $n_{\mathrm{u,d}}$ for each spin channel, the electron entropy is given by [25]

$$S_{\mathrm{el}} = -k_{\mathrm{B}}\int_{-\infty}^{\infty}[f(\ln f) + (1-f)\ln(1-f)](n_{\mathrm{u}} + n_{\mathrm{d}})dE, \tag{18}$$

where f is the Fermi function and E is the energy. Via thermodynamic integration one obtains the corresponding shift in enthalpy. At elevated temperatures, in addition to a broadening of the Fermi function, the shape of the density of states (DOS) itself changes, something which is not taken into account here. However, we expect that for temperatures up to about $T_{\mathrm{m}}/2$, the current approximation is reasonable. In order to obtain a precise DOS, those calculations were done for 128 atoms, with the tetrahedron method for interpolation over a mesh of $5 \times 5 \times 5$ k points.

B. The paramagnetic state

Treating magnetic disorder from first principles is not straightforward in systems containing defects and structural relaxation. In Refs. [7,26] the spin-wave methodology was used. Here we address the problem by averaging over randomly generated spin states in supercell calculations. Starting from structures relaxed in the ferromagnetic state, a set of calculations were carried out without further structural relaxation, but with disordered spins. The initial magnetic moments were set to two Bohr magnetons per atom, and the orientations were set randomly with the constraint that the total magnetic moment be equal to zero in the bulk system. In the vacancy and transition state systems, the number of atoms is odd, and the initial total magnetic moment will thus be two Bohr magnetons.

In order to minimize the statistical error in calculated defect properties the spin structure for the vacancy and transition state systems were the same as in corresponding bulk systems with one atom missing. The averaging over spin states was then done for defect properties as defined in Eqs. (3), (4), and (5).

During the electronic relaxation carried out in VASP both the magnitude and the orientation of the spins were allowed to vary. In the case that a spin is flipped, the above method of averaging becomes invalid. We therefore discarded such calculations, and from originally 80 separate calculations

we could keep 41 sets of data for calculating the diffusion activation energy Q by Eq. (5), and 35 sets of data for calculation of the vacancy formation and migration enthalpies by Eqs. (3) and (4).

C. Spin lattice simulations

In order to investigate how $G^{\mathrm{mag}}(T)$ varies between the low-temperature ferromagnetic and the high-temperature paramagnetic states, we carried out a series of Monte Carlo (MC) simulations within the classical and the quantum Heisenberg models. The basic Hamiltonian to be studied is

$$E = -\sum_{i \neq j} J_{ij} \bar{s}_i \bar{s}_j. \tag{19}$$

Here $\bar{s}$ represent either classical spin vectors, or quantum spin operators. Simulations were carried out using the ALPS package [27], and in the case of classical simulations also using our own code. Interactions J_{ij} up to nearest neighbor (nn) or next-nearest neighbors (nnn) were taken into account. In the case of nn, one single parameter J_0 defines the systems; for the vacancy system, eight interactions are cut, and in the transition state, another seven are cut while six are reformed (representing the six nearest neighbors of the jumping atom). In the case of nnn interactions, an expression is needed for the interaction strength as a function of distance $J(r)$. We used the relation in Ref. [28],

$$J_{ij}(r_{ij}) = J_0 A \left(1 - \frac{r_{ij}}{r_{\mathrm{c}}}\right)^3 \Theta(r_{\mathrm{c}} - r_{ij}). \tag{20}$$

Here $r_{\mathrm{c}} = 3.75$ Å and Θ is the Heaviside step function. The normalizing factor A was introduced by us to make the cohesive energy equal to $4J_0$, as in the nn model. Structural relaxation was not considered in the spin lattice simulations.

For most MC simulations, a system of $8 \times 8 \times 8$ lattice sites was used. Typically, 10^6 MC sweeps were used for thermalization, and 10^7 sweeps for data collection. In the classical simulations, spins were updated by random reorientation, while in the QM simulations, the loop algorithm [29] was used. The calculated critical temperature was obtained as $T_{\mathrm{C}} = 2.05 J_0/k_{\mathrm{B}}$ in the classical nn bulk system, in agreement with previous studies [30].

IV. RESULTS

A. First-principles calculations of diffusion parameters

Calculated vacancy formation and migration activation enthalpies are presented in Table I for the ferromagnetic and the paramagnetic states. The ferromagnetic calculations are in general agreement with previous calculations. Experimental data on vacancy formation are based mainly on Doppler-broadening positron annihilation studies for which the contribution from vacancies is very difficult to distinguish in the ferromagnetic region. Therefore, the experimental value of $H_{\mathrm{f}}^{\mathrm{FM}}$ is somewhat uncertain. The migration enthalpy, on the other hand, is measured by electrical resistivity changes in annealing experiments at $T \approx 400$ K, i.e., well into the ferromagnetic region. The current result ($H_{\mathrm{m}}^{\mathrm{FM}} = 0.69$ eV) is in good agreement with the recent analysis by Tapasa *et al.* [31], as well as with previous first-principles calculations [6,7,32,33].

By averaging over randomly generated spin structures we estimated the paramagnetic vacancy formation and migration enthalpies $H_{\mathrm{f}}^{\mathrm{PM}}$ and $H_{\mathrm{m}}^{\mathrm{PM}}$ according to Eq. (3) and (4), and the paramagnetic migration energy Q^{PM} according to Eq. (5). The distributions of energies in the respective cases are shown in Fig. 1, where Gaussian kernel smoothing with a standard deviation of 0.3 eV was applied. The enthalpies calculated for the PM state can be compared with previous results based on spin-wave calculations. The vacancy migration enthalpy agrees with that in Ref. [7], while our estimate of the vacancy formation enthalpy is significantly lower than that in Refs. [7,26].

There are multiple peaks seen in the energy distributions in Fig. 1. At this stage, it is not clear if this is due to statistical fluctuations or if there is any physical significance to the peaks. In the latter case, it would probably be linked to the local spin structure around the vacancy and transition state, respectively.

B. The electronic contribution

In earlier studies of vacancy formation and migration in the group-VI metals, the electronic contribution to the activation enthalpies was shown to play an important role [35]. In the present study, this contribution was computed based on the 0 K density of states as described in Sec. III A. For the bulk system, we find that the calculated electronic contribution to the thermal capacity is well described by a second-order

TABLE I. Calculated diffusion activation parameters compared with other calculations and experimental data when available. Energies are in eV, entropies in k_{B}, attempt frequency ν_0^* in THz, and the diffusion prefactor D_0 is given in m^2/s.

	Ferromagnetic						Paramagnetic		
	H_{f}	H_{m}	Q	S_{f}	ν_0^*	D_0	H_{f}	H_{m}	Q
54 atoms	2.15	0.69	2.84	4.37	12.7	5.85×10^{-5}	1.54 ± 0.16	0.40 ± 0.17	1.97 ± 0.2
128 atoms	2.17	0.70	2.87	4.83	11.6	8.46×10^{-5}			
Experimental data									
Ref. [34]	2.0 ± 0.2		2.87				1.79 ± 0.10		
Ref. [31]		0.65				2.3×10^{-5}			
Other theoretical results									
Ref. [26]	2.26						1.77		
Ref. [7]	2.13	0.64	2.77				1.98	0.43	2.41

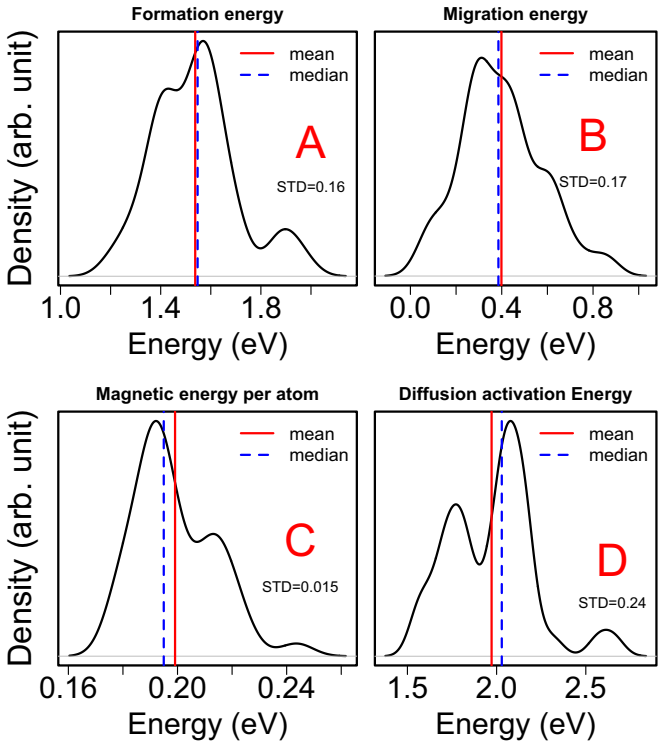

FIG. 1. (Color online) The distribution of energies in the paramagnetic calculations of (a) the vacancy formation enthalpy and (b) the vacancy migration enthalpy. The lower panels show (c) the bulk enthalpy per atom and (d) the diffusion activation enthalpy. The results are based on averaging over 35–40 random spin states, and Gaussian smearing has been applied for visualization. Solid lines and dashed lines represent the mean values and median values, respectively, in each data set.

function $c_{\rm el} = c_2 T^2$ with $c_2 = 2.1 \times 10^{-8}$ eV/K^2. This is in fair agreement with the fit to experimental data in Ref. [36], $c_2 = 3.35 \times 10^{-8}$ eV/K^2, considering the approximations involved.

For diffusion activation in bcc Fe, we find that the term stemming from electronic excitations is relatively small compared to the magnetic contribution in line with findings in Ref. [6]. We have assumed that the electronic contribution as calculated here, i.e., $Q_{\rm el} = Q_2 T^2$, with $Q_2 = 1.1 \times 10^{-7}$ eV/K^2, captures the essential part of the second-order term of $Q(T)$.

C. Heisenberg model Monte Carlo simulations

The classical and quantum Heisenberg models were employed to study the temperature variation of $H_{\rm f}^{\rm mag}$ and $Q^{\rm mag}$. Starting with the bulk calculations, the magnetic enthalpy per atom is shown in Fig. 2. The data were scaled so that the classical disordering enthalpy $\Delta h^{\rm FM\rightarrow PM}$ corresponded to the one obtained in the current DFT calculations: 0.20 eV/atom. From that, the Curie temperature is found to be approximately 1140 K in the case of the quantum MC (QMC) calculations, i.e., within 10% of the experimental value. The experimental magnetic enthalpy $h^{\rm mag}(T)$, as obtained by subtracting other contributions such as phonons and electronic excitations [36],

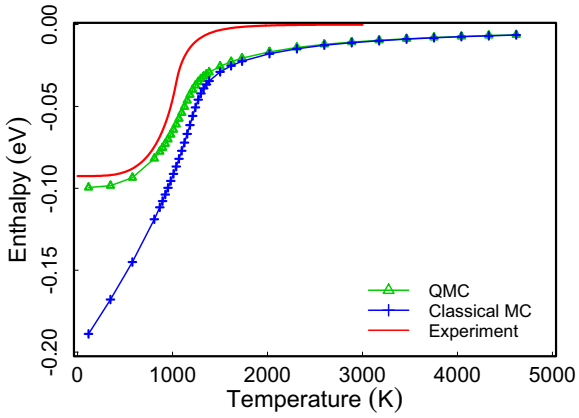

FIG. 2. (Color online) Bulk magnetic enthalpy from classical and quantum MC simulations. The experimental curve [36] based on heat capacity measurements is included for reference.

is also inserted in Fig. 2. One notes that the experimental curve saturates more rapidly above $T_{\rm C}$ compared to the classical or quantum MC ones, which remain below zero even at temperatures several times higher than $T_{\rm C}$. Although such high temperatures are well into the molten region, it shows that there is an inconsistency in the current understanding of the separate effect of spin disordering in Fe.

The difference between the enthalpies obtained in classical and quantum MC at zero temperature corresponds to the magnetic zero-point energy, and equals a half of the total disordering enthalpy. A corresponding term is expected also for the defect parameters, and one should be careful to distinguish between the classical and quantum FM states. In the latter, magnetic fluctuations are present also at 0 K.

The calculated magnetic vacancy formation enthalpy is presented in Fig. 3 along with estimates based on the scaling model, Eq. (13), and the Zener model, Eq. (14). It is seen that the scaling model describes the enthalpy well up to and somewhat above $T_{\rm C}$, while the Zener model gives a somewhat

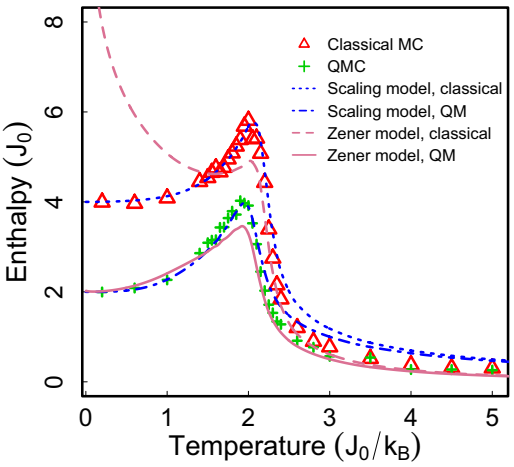

FIG. 3. (Color online) The magnetic part of the vacancy formation enthalpy calculated using MC simulations based on the classical and quantum mechanical Heisenberg model. Solid and dashed lines refer to the scaling and shift (Zener) models, respectively.

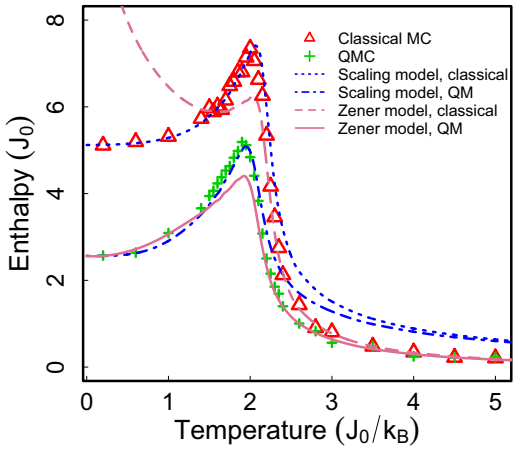

FIG. 4. (Color online) The magnetic part of the diffusion activation enthalpy calculated using MC simulations based on the classical and quantum mechanical Heisenberg model. Solid and dashed lines refer to the scaling and shift (Zener) models, respectively.

better description in the PM region, in terms of enthalpy difference. However, the Zener model becomes nonphysical in the limit $T \to 0$, which is most clearly seen in the classical result, where H_f deviates.

We note that the 0 K vacancy formation enthalpy contains a magnetic zero-point energy term which is negative, i.e., the classical enthalpy is larger than the quantum mechanical one. Since the classical and quantum mechanical results differ substantially below T_C, it is important to distinguish between the two when first-principles results are compared with experimental findings. For instance, the current first-principles results for H_f^{FM} correspond to the classical case, while fits to experiments include quantum mechanical effects below T_C. We will distinguish between the two cases by the superscript "cl" or "qm," respectively.

The calculated magnetic diffusion activation enthalpy $Q^{mag}(T)$ is shown in Fig. 4. As seen, within the current model of distance-dependent interaction parameters J_{ij}, Q^{mag}/H_f^{mag} is close to the expected fraction 5/4 discussed in Sec. II.

The Heisenberg model applied here corresponds to the case $\gamma = 1$, i.e., the formation of a vacancy corresponds to the cutting of the surrounding magnetic interactions, without further modification of the interactions. Consequently, one finds that the predicted 0 K vacancy formation energy H_f^{mag} equals $\Delta h^{FM\to PM}$, both in CMC and QMC calculations. In the classical case this follows immediately from considering the static energy of forming a vacancy. By contrast, typical results based on DFT calculations or on experimental facts (see Table I), imply that $H_f^{mag} \gtrsim 2\Delta h^{FM\to PM}$, suggesting that formation of a vacancy is associated with weakening of the local interactions surrounding it, in addition to the bond-cutting effect itself.

D. Comparison with experimental diffusion data

Having calculated the ferromagnetic parameters (activation enthalpies and prefactors), as well as the electronic and magnetic contributions, we could in principle compare calculated and experimental values of $D(T)$ directly. However, it turns out that this approach does not lead to a good description of experimental diffusion rates, neither quantitatively nor qualitatively. There are a number of reasons for this. First, as discussed, e.g., in Refs. [10,16], the Heisenberg model does not describe the magnetic free energy realistically enough, see also Fig. 2. Instead, we use the fact that the scaling model describes quite well the magnetic part of the vacancy formation and migration free energies, in particular it is straightforward to connect it with static 0 K first-principles results via Eq. (15). Therefore, we combine Eqs. (2) and (13) and take $h(0,\tau)$ from the bulk magnetic enthalpy as measured experimentally and parametrized in Ref. [36]. Second, we expect errors in the calculated parameters Q^{FM} and γ, and therefore they are taken as fitting parameters. The prefactor D_0 and the second-order term Q_2, on the other hand, are taken from the current calculations since the result is less sensitive to uncertainties in those parameters. For instance, our previous experience shows that vibrational prefactors are much less sensitive to the choice of exchange-correlation functional, compared with the activation energy Q, in the relevant temperature range.

The result of a fit of Eq. (2) to experimental data in the α phase of Fe is shown in Fig. 5, with $Q^{fit} = 2.91$ eV and $\gamma_a^{fit} = 4.2$. The activation energy is close to the calculated value in Table I, however one must keep in mind that the calculated value $Q^{FM,cl}$ refers to the classical FM state. Based on the current DFT calculations, a zero-point energy of approximately 0.4 eV should be *subtracted* before a comparison is made with $Q^{FM,qm}$ from experiments.

From the fit we also find $\Delta Q^{FM\to PM,qm} = 0.42$ eV, to be compared with the result from the current DFT calculations, 0.40 eV, where we have used the fact that $\Delta Q^{FM\to PM,cl} = 2\Delta Q^{FM\to PM,qm}$ for localized spins with $S = 1$. Thus, we find that the experimentally estimated $\gamma_a^{fit} = 4.2$ is reasonably close to the theoretical value found here, $\gamma_a = 4.0$. Using this theoretical value and fitting Q gives a result which is virtually identical to that in Fig. 5. However, since there are fairly large

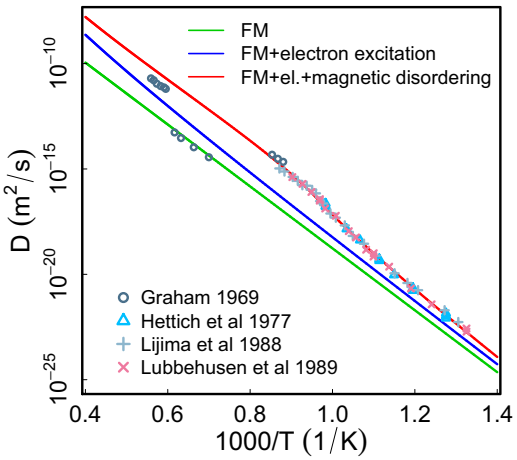

FIG. 5. (Color online) Experimental diffusion data together with a two-parameter fit of the current diffusion model (see text). The fit was done for data in the ferromagnetic α region and slightly above ($T < 1185$ K). The deviation between the fitted line and experimental data in the high-temperature bcc phase (δ-Fe) is within a factor of 3.5, which can be seen as a measure of the quality of the model. The experimental data can be found in Refs. [37–40].

statistical uncertainties in our estimate of γ_a, we prefer not to use it as a fixed parameter.

In the fit shown in Fig. 5, only data in the α region below 1185 K were used. The deviation between the fitted curve and experimental data in the bcc δ phase above 1667 K is within a factor of 3.5, which can be seen as a measure of the quality of the model.

The role of the Heisenberg model simulations in the current work is twofold. First, the simulations suggest that the scaling model can be applied to describe vacancy formation and diffusion activation. It has the advantage over the Zener model that the parameter γ_a can be deduced directly from first-principles calculations of the disordering enthalpy $\Delta Q^{\mathrm{FM}\to\mathrm{PM}}$, by Eq. (15). A corresponding relation applies for the formation enthalpy. Second, the current simulations demonstrate clearly that the quantum mechanical solution for the spin system, and the corresponding zero-point magnon energy, substantially influence the results below T_C and must be accounted for. Specifically, defect formation and diffusion activation energies obtained in standard DFT calculations are not the same as those inferred from experimental data. A similar effect exists for phonon excitations below the Debye temperature T_D. However, since T_D is around room temperature in most metals and alloys, this effect rarely shows up in diffusion data and one can stick to a classical treatment of the phonon free energy.

V. CONCLUSIONS

The magnetic contribution to the vacancy formation and migration free energies in bcc Fe has been investigated. The current first-principles random-spin calculations can be directly compared with previous spin-wave calculations. Reasonable agreement is obtained for the magnetic part of the vacancy migration enthalpy, while the current calculation gives a somewhat lower value of the corresponding formation enthalpy. The issue is worth further investigation, especially since the sum of the two $\Delta Q^{\mathrm{FM}\to\mathrm{PM,qm}}$ obtained here corresponds to typical values based on fits to experiments.

Our simulations based on a next-nearest neighbor Heisenberg model provide a description of the shape of the magnetic part of the diffusion activation free energy, in the temperature range of the FM to PM transition. However, this simplified model does not take into account that the effective spin interactions are long ranged and also dependent on the global spin order. Therefore, a semiempirical model has been used in this work to fit experimental self-diffusion data. The result of this fit can be compared with first-principles estimates of the magnetic part of the diffusion activation enthalpy, specifically $\Delta Q^{\mathrm{FM}\to\mathrm{PM}}$ via Eq. (15). Although the statistical uncertainty in the current theoretical estimate of $\Delta Q^{\mathrm{FM}\to\mathrm{PM}}$ is substantial, a coherent picture still emerges. The shift in activation enthalpy between the FM and the PM states is roughly four times the bulk disordering enthalpy, i.e., $\gamma_a \approx 4$. Within a Heisenberg model with fixed spin interactions, this value is expected to be roughly 1. Therefore, we draw the conclusion that the local spin interactions are weakened when the vacancy or the activated state are formed. It would be of great interest to check this result against more detailed DFT calculations.

Finally, we point out that the FM vacancy formation enthalpy, migration enthalpy, and diffusion activation enthalpy all contain a contribution due to quantum mechanical fluctuations, also at 0 K (the zero-point magnon energy). This term needs to be accounted for when DFT calculations are compared with experiments. Our estimate is that the diffusion activation enthalpy, as well as the vacancy formation enthalpy, calculated from first-principles DFT within the GGA, are underestimated with about 10%. This would be in line with what has been found in other metals such as Al and Mo [5,41].

ACKNOWLEDGMENTS

This work was funded by the Swedish Research Council through the project GENIUS, by the Göran Gustafsson Stiftelse and by the European Commission under the Euratom Theme of the 7th Framework Programme for Research and Technological Development under Grant Agreement No. 604862 (MatISSE) and in the framework of the EERA (European Energy Research Alliance) Joint Programme on Nuclear Materials. The high-performance computing resources were provided by the Swedish National Infrastructure for Computing (SNIC).

[1] N. Sandberg, B. Magyari-Kope, and T. R. Mattsson, Phys. Rev. Lett. **89**, 065901 (2002).
[2] N. Sandberg and R. Holmestad, Phys. Rev. B **73**, 014108 (2006).
[3] M. Mantina, Y. Wang, R. Arroyave, L. Q. Chen, Z. K. Liu, and C. Wolverton, Phys. Rev. Lett. **100**, 215901 (2008).
[4] D. Simonovic and M. H. F. Sluiter, Phys. Rev. B **79**, 054304 (2009).
[5] T. R. Mattsson, N. Sandberg, R. Armiento, and A. E. Mattsson, Phys. Rev. B **80**, 224104 (2009).
[6] S. Huang, D. L. Worthington, M. Asta, V. Ozolins, G. Ghosh, and P. K. Liaw, Acta Mater. **58**, 1982 (2010).
[7] H. Ding, V. I. Razumovskiy, and M. Asta, Acta Mater. **70**, 130 (2014).
[8] L. Messina, M. Nastar, T. Garnier, C. Domain, and P. Olsson, Phys. Rev. B **90**, 104203 (2014).
[9] B. Jonsson, Z. Metallkd. **83**, 349 (1992).
[10] F. Kormann, A. Dick, T. Hickel, and J. Neugebauer, Phys. Rev. B **81**, 134425 (2010).
[11] S. Glasstone, K. J. Laidler, and H. Eyring, *The Theory of Rate Processes* (McGraw-Hill, New York, 1941).
[12] G. H. Vineyard, J. Phys. Chem. Solids **3**, 121 (1957).
[13] L. A. Girifalco, J. Phys. Chem. Solids **23**, 1171 (1962).
[14] L. A. Girifalco, J. Phys. Chem. Solids **25**, 323 (1964).
[15] M. Schoijet and L. A. Girifalco, J. Phys. Chem. Solids **29**, 481 (1968).
[16] R. Braun and M. Feller-Kniepmeier, Scr. Metall. **20**, 7 (1986).
[17] T. Nishizawa, M. Hasebe, and M. Ko, Acta Metall. **27**, 817 (1979).
[18] C. Zener, Trans. AIME **203**, 619 (1955).
[19] G. Kresse and J. Hafner, Phys. Rev. B **47**, R558 (1993).
[20] G. Kresse and J. Hafner, Phys. Rev. B **49**, 14251 (1994).
[21] G. Kresse and J. Furthmüller, Phys. Rev. B **54**, 11169 (1996).

[22] P. E. Blöchl, Phys. Rev. B **50**, 17953 (1994).
[23] G. Kresse and D. Joubert, Phys. Rev. B **59**, 1758 (1999).
[24] V. Ozolins, B. Sadigh, and M. Asta, J. Phys.: Condens. Matter **17**, 2197 (2005).
[25] G. Grimvall, *Thermophysical Properties of Materials*, enlarged and revised ed. (Elsevier, Amsterdam, 1999).
[26] A. V. Ruban and V. I. Razumovskiy, Phys. Rev. B **85**, 174407 (2012).
[27] B. Bauer, L. D. Carr, H. G. Evertz, A. Feiguin, J. Freire, S. Fuchs, and l. Gamper, J. Stat. Mech. (2011) P05001.
[28] P.-W. Ma, C. H. Woo, and S. L. Dudarev, Phys. Rev. B **78**, 024434 (2008).
[29] H. G. Evertz, Adv. Phys. **52**, 1 (2003).
[30] K. Chen, A. M. Ferrenberg, and D. P. Landau, Phys. Rev. B **48**, 3249 (1993).
[31] K. Tapasa, A. Barashev, D. Bacon, and Y. N. Osetsky, Acta Mater. **55**, 1 (2007).
[32] C. Domain and C. S. Becquart, Phys. Rev. B **65**, 024103 (2001).
[33] P. Olsson, C. Domain, and J. Wallenius, Phys. Rev. B **75**, 014110 (2007).
[34] L. DeSchepper, D. Segers, L. Dorikens-Vanpraet, M. Dorikens, G. Knuyt, L. M. Stals, and P. Moser, Phys. Rev. B **27**, 5257 (1983).
[35] A. Satta, F. Willaime, and S. de Gironcoli, Phys. Rev. B **57**, 11184 (1998).
[36] Q. Chen and B. Sundman, J. Phase Equilib. **22**, 631 (2001).
[37] M. Lübbehusen and H. Mehrer, Acta Metall. Mater. **38**, 283 (1990).
[38] Y. Iijima, K. Kimura, and K. Hirano, Acta Mater. **36**, 2811 (1988).
[39] G. Hettich, H. Mehrer, and K. Maier, Scr. Mater. **11**, 795 (1977).
[40] D. Graham and D. Tomlin, Philos. Mag. **8**, 1581 (1963).
[41] K. Carling, G. Wahnström, T. R. Mattsson, A. E. Mattsson, N. Sandberg, and G. Grimvall, Phys. Rev. Lett. **85**, 3862 (2000).